UV-Assisted Lipoic Acid Ligand Exchange of Copper Indium Disulfide-Zinc Sulfide Core-Shell Quantum Dots

by
Lane D. Porth

A PROJECT

submitted to

Oregon State University

University Honors College

in partial fulfillment of
the requirements for the
degree of

Honors Baccalaureate of Science in Chemical Engineering (Honors Scholar)

Presented May 14, 2015
Commencement June 2015

AN ABSTRACT OF THE THESIS OF

Lane D. Porth for the degree of Honors Baccalaureate of Science in Chemical Engineering presented on May 14, 2015. Title: UV-Assisted Lipoic Acid Ligand Exchange of Copper Indium Disulfide-Zinc Sulfide Core-Shell Quantum Dots.

Abstract approved:

_____

Gregory S. Herman

Water-soluble quantum dots obtained through ligand exchange are widely applicable for biological imaging and marking, LEDs, and photovoltaics. Lipoic acid (LA) was reduced to dihydrolipoic acid (DHLA) using 365-nm soft UV light in a process known as photoligation, and ligand exchange with dodecanethiol-capped $CuInS_2$-ZnS core-shell quantum dots occurred. The reaction was allowed to proceed 24-48 hours when using 50 mM LA in methanol and quantum dots dissolved in hexane. Reaction success was confirmed by continued solubility of quantum dots in methanol following high-speed centrifugation. The product was characterized using UV-visible spectroscopy, photoluminescence, and Raman spectroscopy. Quantum yield decreased from approximately 25% to 3% and a small red shift in peak location was observed after ligand exchange. The process described shows great promise for producing water-soluble quantum dots. Functionalization and end uses can be explored following additional experiments to improve water solubility and quantum yield.

Key Words: quantum dots, ligand exchange, lipoic acid, photoligation

Corresponding e-mail address: laneporth@gmail.com

UV-Assisted Lipoic Acid Ligand Exchange of Copper Indium Disulfide-Zinc Sulfide Core-Shell Quantum Dots

by
Lane D. Porth

A PROJECT

submitted to

Oregon State University

University Honors College

in partial fulfillment of
the requirements for the
degree of

Honors Baccalaureate of Science in Chemical Engineering (Honors Scholar)

Presented May 14, 2015
Commencement June 2015

Honors Baccalaureate of Science in Chemical Engineering project of Lane D. Porth presented on May 14, 2015.

APPROVED:

Gregory S. Herman, Mentor, representing Chemical, Biological, and Environmental Engineering

Líney Árnadóttir, Committee Member, representing Chemical, Biological, and Environmental Engineering

Majid Ahmadi, Committee Member, representing Chemical, Biological, and Environmental Engineering

Toni Doolen, Dean, University Honors College

I understand that my project will become part of the permanent collection of Oregon State University, University Honors College. My signature below authorizes release of my project to any reader upon request.

Lane D. Porth, Author

Acknowledgements

I do not think it would be possible for me to properly thank everyone who has assisted me on this project, in my education, or throughout my life. I will give it my best effort. Many who did much will not be on this list.

- Thank you to my parents and family for all of your support emotional, financial, and otherwise, raising me well, and teaching me how to work hard.
- Thank you to Prof. Herman for your willingness to serve as my thesis mentor and all your advice and teaching over the past four years.
- Thank you to Majid for all of your help with the ligand exchange project. I would not have been able to complete this thesis without your help. Thank you for providing quantum dots and assisting with characterization.
- Thank you to Prof. Árnadóttir for your willingness to sit on my thesis committee.
- Thank you to Steve Wuerch for your inspiration throughout the years. My life was changed when I walked into Pre-Chemistry for the first time in 8th grade.
- Thank you to everyone in the Herman Group (past and present) for your assistance and sharing space. Meena, Jaana, Charith, Richard, Brendan, Bob, and Gustavo, you have all helped me on my way.
- Thank you to my fiancée Cassie for your moral support throughout this process. Not many people would be willing to put up with me and my homework load.
- Thank you to all of my friends in CBEE. You are all great. Audrey, Nathan, Alyson, Chelsea, Stefanie, Madi, Larkin, Linda, and Liz, I will remember all the fun memories and late-night study sessions we had together.

Table of Contents

List of Figures

List of Tables

UV-Assisted Lipoic Acid Ligand Exchange of Copper Indium Disulfide-Zinc Sulfide Core-Shell Quantum Dots

1. Introduction

1.1 Quantum Dot Applications

Quantum dots are semiconductor nanocrystals that are so small they exhibit quantum characteristics that can be modeled by the one-dimensional particle-in-a-box model suggested by quantum mechanics. This creates properties not observed in a bulk semiconductor material with the same composition chief of which is fluorescence that can be tuned by varying the composition and size of the nanoparticles down to dimensions of the exciton Bohr radius. [1] [2] [3] [4] Quantum dots have various and increasing applications that include LED lighting, photovoltaics, lasers, biological marking, and biological imaging. [1] [2] [3] [4] [5] [6] [7] [8] [9] [10] [11] [12] Synthesis generally takes place using metal salt precursors and coordinating long-chain solvents resulting in quantum dots that are capped with long-chain hydrocarbon ligands leaving them soluble only in non-polar organic solvents such as toluene or hexane. A ligand exchange reaction must be performed to transfer the quantum dots into aqueous media for use in solar or biological applications where solubility in water may be useful for deposition in photovoltaic applications or non-toxicity in biological applications. Biological marking and imaging applications require additional surface functionalization after

the ligand exchange reaction to target the quantum dots to a specific organ or system for imaging or to a tumor to assist surgeons in removal. [1] [5] [6] [8] [11]

1.2 Ligand Exchange

Quantum dots are generally capped with hydrophobic ligands and suspended in organic, non-polar solvents after synthesis. Two common capping ligands are trioctylphosphine (TOP) and trioctylphosphine oxide (TOPO). Another common capping ligand is dodecanethiol (DDT). It is desirable to replace these hydrophobic ligands with multidentate hydrophilic ligands that can be further functionalized to target specific tissues or surfaces. [1]

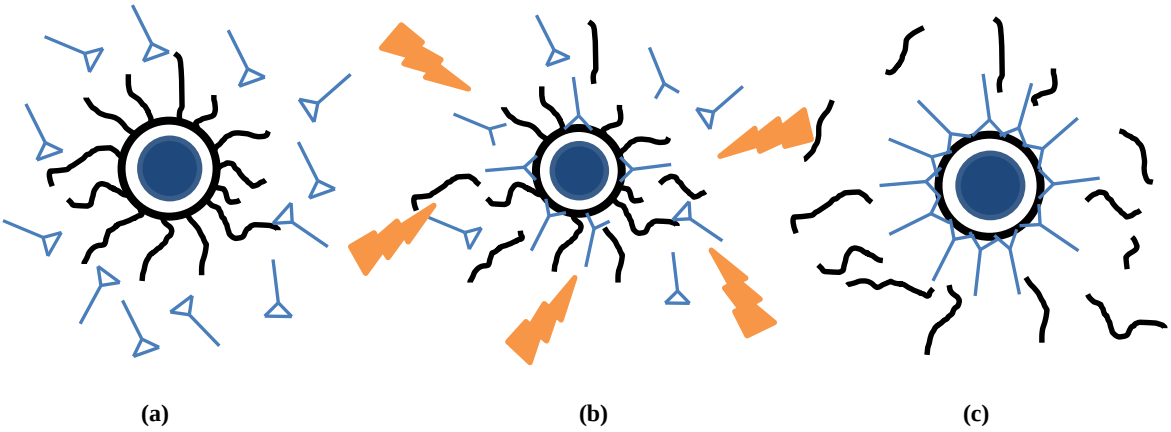

Figure 1: Schematic showing the ligand exchange process for the lipoic acid/dihydrolipoic acid (LA/DHLA) system described later in more detail. **(a)** A quantum dot capped with hydrophobic ligands in a non-polar organic solvent is brought in close contact with LA. **(b)** UV light is used to reduce LA into DHLA which can then replace hydrophobic ligands on the quantum dot surface. The transfer is incomplete in this figure. **(c)** A quantum dot shown after the ligand exchange is complete. The nanoparticle is now soluble in water. Figure adapted from **[1]**.

A simple schematic of the ligand exchange process for a lipoic acid/dihydrolipoic acid (LA/DHLA) system is shown in **Figure 1**. The process, known as photoligation, uses UV light to reduce LA to DHLA which is then able to displace the TOP/TOPO or DDT capping ligand on the surface of the core-shell quantum dot [1] [6]. Other ligand exchange processes use hours of vigorous stirring

catalyzed by high solution pH to carry out ligand exchange. [3] [5] [13] Yet other groups reported heating the high pH mixture to drive ligand exchange. [2]

Additional functionalization steps are necessary following the ligand exchange process depending on the desired application. This conjugation process is especially important for biological applications where the quantum dots must be concentrated within a certain tissue to allow for imaging or treatment. Reports have shown that bioconjugation significantly enhances tissue targeting and the corresponding images obtained. [8] **Table 1** provides a list describing several functionalized quantum dot systems.

Table 1: Summary of several quantum dot applications following ligand exchange. The ligand used and information regarding further functionalization are listed.

Application	Ligand	Functionalization	Source
In-vitro pancreatic cancer imaging	LA/DHLA	2A3 antibody	[8]
In-vivo brain tumor imaging	11-mercaptoundecanoic acid (MUA)	EG2 antibody	[8]
Brain capillary imaging	LA/DHLA-based	Polyethylene glycol (PEG)-OCH_3, PEG-COOH, PEG-NH_2, and zwitterion	[1]
Sensitized solar cells	3-mercaptopropionic acid (MPA)	No additional functionalization	[5]
Cellular imaging	LA/DHLA	PEG	[6]
Renal imaging	LA/DHLA and cysteine	PEG or no further functionalization	[11]
Lymph node imaging	LA/DHLA	PEG and PEG-COOH	[9]
Light-emitting transistor	MPA	Oleic acid	[10]
Fluorescent tagging	LA/DHLA	Maltose binding protein	[12]

Another consideration when using quantum dots in biological applications is toxicity. These concerns must be addressed in other applications when considering the environmental impact of quantum dots. Much like other nanoparticles, the effects of quantum dots on living organisms are not well known. One report stated that no "obvious cytotoxic effects on tissue" were noticed throughout a two-day test period, while another review reported varying results for CdSe-ZnS quantum dots, but more rigorous toxicity studies need to be performed. [6] [14] Factors to consider in

producing non-toxic quantum dot applications include the presence of residual organic solvents such as methanol or hexane, the metals used to produce the quantum dots (many metals such as cadmium are well-known to be toxic), and renal clearance of quantum dots once their useful life has been exhausted. [9] [11] Renal clearance is important as regulatory authorities such as the United States Food and Drug Administration often require full clearance of foreign agents to reduce the risk of any toxic effects. This requirement will pose a technical challenge as many of the quantum dot systems currently being explored were found by one group to have hydrodynamic diameters greater than the 5.5-nm limit that allows for efficient removal through urination. [11]

1.3 Candidates for Ligand Exchange

Many different methods are available to functionalize quantum dots once they have undergone ligand exchange, but relatively few ligands have been reported on for the exchange itself. Ligands used for exchange must fulfill several conditions beginning with possessing characteristics allowing the ligand to interact with both the surface of the quantum dot and the surrounding water. [1] [6] Other important characteristics include small hydrodynamic size for easy renal clearance; high affinity for the quantum dot surface (bidentate or multidentate); receptivity to conjugation with proteins, antibodies, or other molecules to allow for targeting; and stability in solutions including biological buffers at varying pH and ionic strength. The most common ligands use thiol groups to attach to the surface of the quantum dot shell, but other terminal groups such as amines, phosphonic acids, and carboxylic acids have been used. The other end of the ligand's hydrocarbon backbone consists of

deprotonated carboxylic acids, alcohol groups, methoxy groups, or amines which can be soluble in water or conjugated with a targeting protein or antibody. [15] [16] Several examples are listed in **Table 1**.

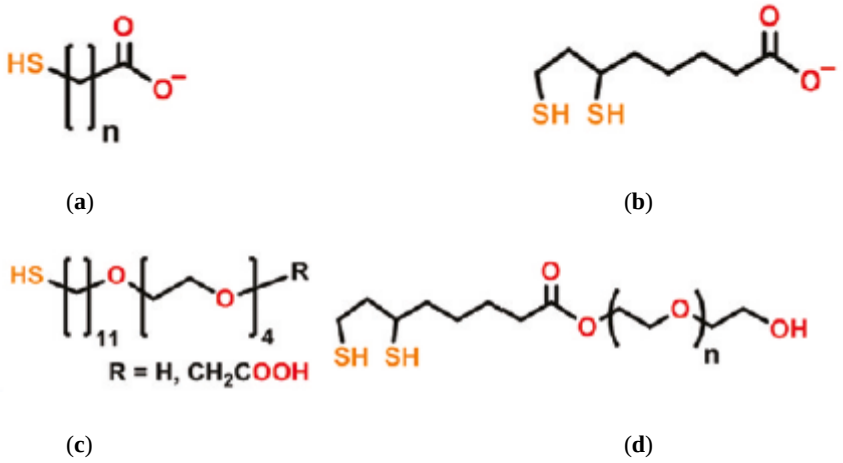

Figure 2: Molecular structures of two common types of ligands and their PEG derivatives. (**a**) Thioalkyl acid ligand which would be MPA when n=2 or MUA when n=10. This ligand is negatively charged. (**b**) DHLA after reduction from LA and ring opening. DHLA is also negatively charged. (**c**) PEGylated ligand based on a thioalkyl acid backbone. This system has no charge and is easily conjugated. (**d**) PEGylated DHLA-based ligand. This system is also neutral and more easily conjugated. Images taken from **[15]**.

The majority of existing reports on quantum dot ligand exchange detail thioalkyl acids or DHLA and their derivatives. Examples of these ligands are displayed in **Figure 2**. Many of the thioalkyl acid reports focus on ligand exchange using MPA and corresponding applications. [3] [5] [10] [13] MUA is another thioalkyl acid commonly used for ligand exchange, and several others are mentioned in review papers including 4-mercaptobenzoic acid and 2-mercaptoacetic acid. [2] [8] [14] [15] [16]. The structure of a general thioalkyl acid is pictured in **Figure 2a**. DHLA is the basis of the second major group of cap exchange ligands. Unfunctionalized DHLA carries a negative charge and is not targeted to any specific tissue (structure pictured in **Figure 2b**), so it is often connected to PEG of varying molecular weights to produce a neutral ligand and functionalized to target a specific

tissue such as a cancerous tumor or a vascular structure for imaging (see **Figure 2d** for chemical structure). [1] [6] [7] [8] [9] [12] DHLA-based ligands can also be zwitterionic possessing both positive and negative charges on the same molecule. A final ligand family that has received some attention is cysteine and other similar ligands including cysteamine. They have the advantage of a smaller hydrodynamic size, but they suffer from much shorter shelf lives and less stability in solution than other ligands under consideration. [11] [16]

1.4 Lipoic Acid and Dihydrolipoic Acid Ligand Exchange

DHLA exhibits many of the characteristics of an ideal hydrophilic capping ligand. Its specific advantages over the more commonly used thioalkyl acids include two sites to bond to the quantum dot surface, greater stability in solution including a longer shelf life, and relatively small hydrodynamic diameter. DHLA is also easily conjugated to lend even greater stability in solution across a wide pH range and provide functionalization to target specific tissues. [1] [6] [7] [15] [16] It is also more likely to lead to non-toxic applications, as it is derived from LA which is a common dietary supplement. [17] DHLA is not without disadvantages. Thioalkyl acids are usually easier to obtain commercially than DHLA and less sensitive to the environment in which they are handled. DHLA, when not conjugated, is sensitive to solution pH beginning to come out of solution under mildly acid conditions. [6] [7] [12] [16]

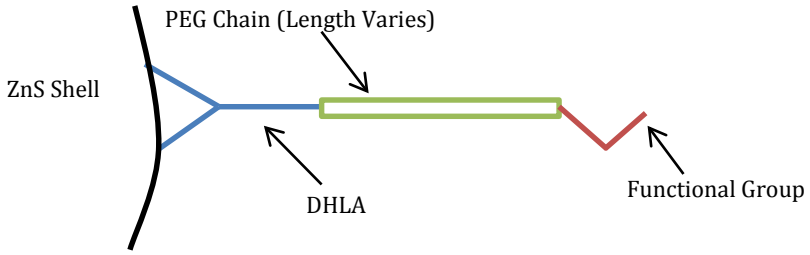

Figure 3: Simple schematic depicting DHLA attached to a quantum dot shell and functionalized using PEG and a group such as $–OCH_3$, $-NH_2$, or –COOH. The PEG segment provides greater stability at a variety of pH and ionic strengths while the end group allows for targeting to a specific application. Adapted from **[1]** and **[16]**.

The primary solution to the colloidal instability of DHLA is conjugation with a PEG chain. This also serves to neutralize the negative charge of DHLA (see **Figure 2**) and makes further functionalization for targeting specific tissues easier. A simplified schematic showing a functionalized quantum dot is shown in **Figure 3**. [1] [6] [7] [15] Adjusting the solution pH can also increase the water solubility of DHLA-coated quantum dots. [1] [6] [12] The tradeoff of increased colloidal stability from conjugation is increased hydrodynamic diameter. A balance must be struck between small hydrodynamic size and colloidal stability which will be unique to each application. [11] [16]

In the past, many groups synthesized their own DHLA ligands to circumvent short shelf life and lack of commercial availability. This process involved synthesis of LA (including any functional groups desired), reduction using sodium borohydride, and then ligand exchange at temperatures 60-70 °C. [6] [8] [11] [12] This method, while effective, introduced additional problems because of the ease with which DHLA can reoxidize back to a disulfide and the reactivity of sodium borohydride which can damage some functional groups used for conjugation. [1] Mattoussi's group developed a method known as photoligation to avoid this difficulty by

producing DHLA in-situ from LA which can be purchased commercially or synthesized in the lab. While LA is still a sensitive compound, many of the handling difficulties associated with DHLA are eliminated by the photoligation method. [1] [7] [18]

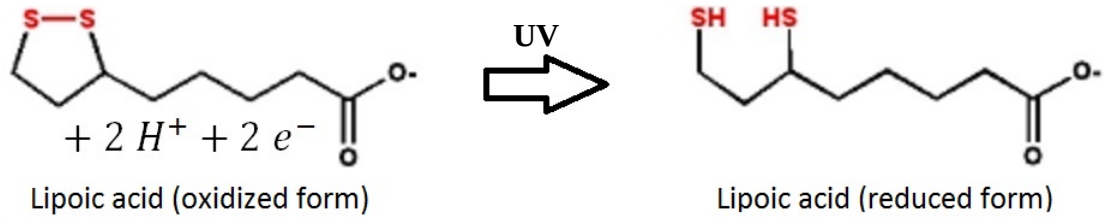

$$LA + 2\,H^+ + 2\,e^- \rightleftarrows DHLA$$

Figure 4: The ring-opening reduction of LA to DHLA in the presence of UV light is the basis of the photoligation strategy. Modified image used under a Creative Commons license from UC Davis ChemWiki (http://chemwiki.ucdavis.edu/Biological_Chemistry/Metabolism/Nutrition).

The photoligation strategy replaces the reduction of LA using sodium borohydride with a UV-initiated ring-opening reaction of LA to form DHLA as shown in **Figure 4**. Electrons are provided by a UV light source through excitation of LA and react with two protons to reduce LA to DHLA. Some evidence exists to suggest that the quantum dots present in the solution contribute to the reaction by providing an additional source of free electrons and removing products from solution shifting the equilibrium forward. [1] The presence of H^+ as a reactant suggests that performing the reaction in an acidic environment would help drive the reaction, however most reports use strong bases such as sodium hydroxide, tetramethylammonium hydroxide, or potassium *tert*-butoxide to catalyze the reaction or adjust the final solution pH to improve colloidal stability. [1] [7] [18]

The versatility of photoligation is increased by its adaptability to use with engineered DHLA ligands, various solvents, and in either a one- or two-phase

reaction. Mattoussi's group has published multiple reports describing the DHLA-based ligands that have been exchanged using photoligation including PEG-conjugated DHLA, zwitterionic DHLA, bis(DHLA) with four terminal thiol groups, and functionalized DHLA ligands with terminal groups such as $–OCH_3$. [1] [7] [18]. Solvent selection depends on the specific ligand being used and whether a one- or two-phase reaction is being used. Polar solvents used include methanol, ethanol, 1-propanol, 2-propanol, 1-butanol, and *tert*-butanol while hexane was the primary non-polar solvent used. A one-phase reaction type mixes quantum dot precipitate with a polar solvent providing greater flexibility in solvent selection but requiring additional isolation steps after the ligand exchange occurs. Once all reactants have been combined, the UV light source is turned on and the reaction endpoint is reached when all quantum dots have dissolved in the polar solvent. The two-phase ligand exchange process transfers quantum dots from a non-polar solvent such as hexane into a polar solvent like methanol. Ligand exchange is complete when the non-polar solvent no longer contains quantum dots. [1]

2 Materials and Methods

2.1 Materials

The following chemicals were obtained for the ligand exchange reaction. All chemicals were used without further purification except as noted. Lipoic acid (99%) was purchased from Spectrum Chemical Manufacturing Corporation. HPLC-grade methanol (99.8%) and hexanes (98.5%) were obtained from EMD along with ACS reagent-grade acetone from Macron Fine Chemicals and purged with nitrogen gas to remove any dissolved oxygen. The hexanes and acetone were also dried to remove any residual water. Ultra-pure 18.2-MΩ deionized water was used for all steps requiring the addition of water. It was filtered using a disposable 0.2-μm syringe filter and purged with nitrogen gas to remove any dissolved oxygen. The $CuInS_2$-ZnS core-shell quantum dots used for the exchange were capped with dodecanethiol (DDT) and dissolved in hexanes.

Quantum dots were synthesized from the following chemicals. All chemicals were used without further purification. Copper(I) iodide (99.99%), anhydrous indium(III) acetate (99.999%), and diphenylphosphine (99%) were obtained from Alfa Aesar as quantum dot core precursors. Oleic acid (technical grade, 90%) and zinc acetate dihydrate (97%) were also obtained from Alfa Aesar for cation exchange and ZnS shell growth. The solvent and capping ligand for the synthesis was 1-dodecanethiol (≥98%) obtained from Sigma-Aldrich. Elemental sulfur from Fisher Scientific mixed with diphenylphosphine (DPP) served as the sulfur source for core and shell growth. Ultra high purity argon from Airgas was used to provide an inert atmosphere during synthesis.

2.2 Quantum Dot Synthesis

The quantum dot synthesis process began with solution preparation under an inert atmosphere in an mBraun MD10 Compact glove box where 0.06-g CuI and 0.09-g $In(OAc)_3$ were dissolved in 12.4-mL DDT at approximately 100 °C. Diphenylphosphine sulfide (DPPS) was prepared by combining sulfur with DPP at 60 °C. The DPPS was dissolved in 7.6-mL DDT and combined with the copper and indium precursors. The precursors were transferred to a three-neck flask (under argon gas) using a glass syringe and degassed to remove any dissolved oxygen. A peristaltic pump delivered the precursors and argon (to introduce segmented flow) to a Sairem GMP G3 2.45 GHz Microwave Generator where the temperature was maintained between 210 °C and 220 °C. Nucleation began in the microwave zone before the nanocrystals moved to a heating bath kept at 160 °C for growth to continue. The product $CuInS_2$ core quantum dots were collected at the outlet of the continuous process.

Cation exchange and ZnS shell growth began with preparation of 0.7-g $Zn(OAc)_2 \cdot 2H_2O$ and 1.9-g oleic acid in 11.9-g DDT in a three-neck flask. The solution was heated to 60-100 °C and degassed overnight, as the presence of oxygen would damage core integrity. Previously prepared quantum dot cores were added to the solution once it had cooled below 50 °C, and the solution was degassed for several more hours. Cation exchange occurred by introducing zinc precursors to the quantum dot cores when the solution was quickly heated to 250 °C where the temperature was maintained for an hour. Shell growth took place when the temperature was lowered to 210 °C and 0.61-g DPPS (0.6-g DPP and 0.01-g sulfur

powder) in 12.0-g DDT was added. Shell growth took place for 20 hours. The quantum dots were isolated, purified, and dissolved in hexane for ligand exchange.

2.3 Solution Preparation

Ligand exchange reactions were performed using both 50 mM and 100 mM lipoic acid (LA) solutions in methanol. The solutions were prepared under an inert atmosphere in a glove box using solvents that had been purged with nitrogen to remove any dissolved oxygen. More concentrated 100 mM LA was prepared by combining 21-mg LA with 1000-µL methanol. The solution was agitated to ensure a homogeneous solution and used as prepared. This solution was further diluted to produce 50 mM LA by combining 500 µL with 500-µL pure methanol.

The volume of quantum dots dissolved in hexane used for a ligand exchange reaction will depend on the concentration of the solution. The reactions described here used 300-µL concentrated quantum dots in hexane combined with 2000-µL pure hexane. The reaction can be completed with less hexane (successful exchange occurred with 1200 µL), but the additional solvent helps reduce quantum dot precipitation on the wall of the reaction vessel due to evaporation because of slightly elevated temperatures caused by the 365-nm soft UV lamp.

2.4 Ligand Exchange Setup

The ligand exchange reaction employed only simple components in a compact setup. The reaction took place in a 10-mL one-neck flask sealed from oxygen exposure using a 14/20 size septum. A stir bar was inserted while the flask was still under an oxygen-free atmosphere in the glove box. The flask was positioned on a

stirrer using a laboratory stand and clamps so that uniform mixing could be achieved during the reaction.

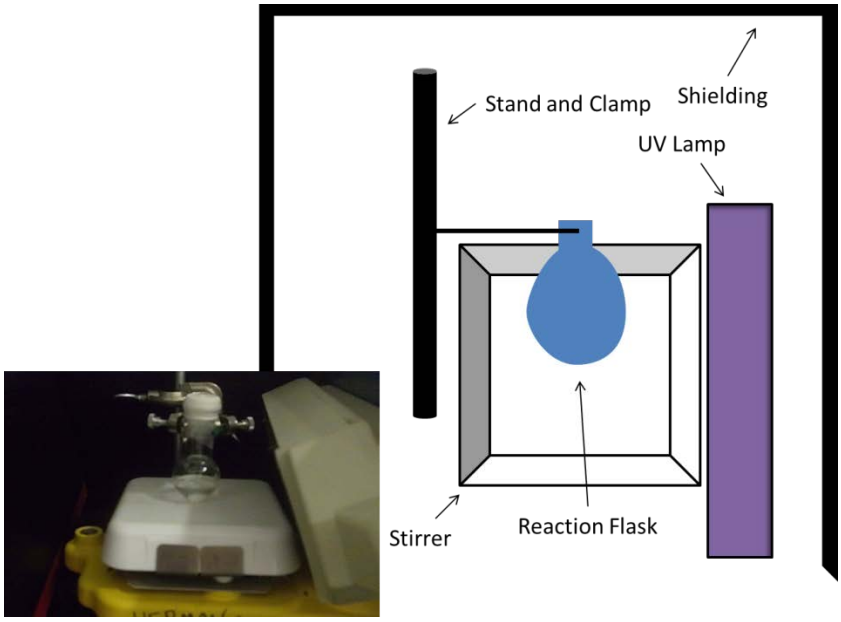

Figure 5: Schematic of experimental setup used for ligand exchange reaction. The equipment and glassware necessary for the reaction are minimal and setup was designed to be quick. A photo of the setup is seen in the inset.

The experimental design, shown in **Figure 5**, was completed by positioning the UVP UVL-56 Handheld UV Lamp to provide full exposure to the reaction components within the flask. The lamp provided 365-nm UV light at 6 W. The full setup is surrounded by black or dark-colored shields to provide for better viewing, image capture, and protection from excess ambient light.

2.5 Ligand Exchange Reaction

The actual ligand exchange reaction proceeded in a straightforward manner. Solution preparation and many of the isolation steps are sensitive and must be performed in a glove box to avoid oxygen exposure, but the reaction itself was completed without any special precautions as long as the reaction flask remained sealed and excessive ambient light exposure was avoided. The main drawback to the

procedure was the long reaction time required for ligand exchange to occur to a satisfactory stage. Reaction times ranged from 24-48 hours under most conditions with variations due to LA and quantum dot concentration. Ligand exchange reactions do not require constant monitoring, so the reaction could be left to proceed overnight and while other work was ongoing with periodic checkups every 4-10 hours to record progress, take pictures, and ensure stable reaction conditions.

(a) **(b)**

Figure 6: (a) Picture taken immediately prior to turning stirrer off to check on reaction progress. **(b)** Picture of reaction showing some quantum dots transferred to the methanol phase. The image was captured after allowing the phases to separate for 15 minutes. The hexane phase forms the top layer.

The reaction began when the UV lamp was turned on and the stirrer was set to its highest setting. This allowed for the methanol and hexane phases of the reaction to be in continuous contact with one another. The reaction was easily interrupted when necessary to take pictures without causing any harm to the process. The best practice was to take images of the reaction in progress prior to switching off the stirrer (shown in **Figure 6a**) then allowing the two phases to separate for 10-15 minutes before taking another picture and resuming the stirring (see **Figure 6b**). The stirrer was switched off and the phases allowed to settle for at least one hour prior to switching off the UV light source and beginning the isolation process.

Figure 7: Image showing agglomerated quantum dots on the wall of the reaction vessel. The agglomeration shown here inside the red circle was not serious enough to warrant adding additional hexane, but it would be beneficial to attempt to wash the deposit off the wall by tilting the flask while stirring.

Two common issues encountered during the course of a reaction are quantum dot agglomeration on the walls of the reaction flask and evaporation of hexane into the headspace above the liquid. Agglomeration of quantum dots on the walls of the flask as seen in **Figure 7** was generally caused by evaporation of hexane into the headspace because of heat from the UV lamp. Quantum dots were resuspended in the liquid phase by simply tipping the flask while on the stirrer temporarily bringing the quantum dots into contact with the hexane-methanol mixture in the flask. This resuspended many but not all of the quantum dots, and additional hexane needed to be added to the reaction to clean the remaining agglomeration off the walls. This activity is relatively high-risk due to the necessary transfer of the reaction vessel to the glove box to add additional hexane (oxygen exposure must still be avoided) and because the reaction must be interrupted for a longer period. This action is not recommended unless a significant portion of hexane has evaporated and a large amount of quantum dots have collected on the walls.

2.6 Isolation and Resuspension

Isolation of the ligand exchange product is the most labor-intensive portion of the process. The need to retain an oxygen-free atmosphere for dihydrolipoic acid (DHLA) necessitates the product to be transferred in and out of the glove box several times to wash and isolate the methanol-soluble quantum dots from impurities. The process began by transferring the reaction vessel containing the final product along with hexane containing residual quantum dots and any byproducts into the glove box. The majority of the hexane phase was removed and discarded, and the methanol phase containing DHLA-functionalized quantum dots was transferred into a glass centrifuge vial. An identical volume of fresh hexane was added to the vial and the lid was securely attached before it was removed from the glove box. The vial was vigorously shaken and then centrifuged in a VWR Clinical 200 Centrifuge for 3 minutes at 3000 rpm. The vial was then carefully transferred back to the glove box where the hexane phase was discarded and the methanol supernatant containing dissolved quantum dots was removed to another centrifuge tube carefully leaving behind any precipitate. The process was repeated two additional times. A reproduction of the full ligand exchange procedure can be found in **Appendix A**.

The purified product dissolved in methanol was used for characterization and attempts to transfer the quantum dots into water using either evaporation or through acetone “crashing.” The first method used a vacuum pump to remove methanol from the quantum dots which were then exposed to oxygen-free 18.2-MΩ distilled water that had been passed through a 0.2-μm syringe filter. Acetone “crashing” required the addition of a comparatively large quantity of acetone followed by centrifugation at

4500 rpm for 15-30 minutes. Acetone disrupted the interaction between DHLA and methanol and caused the quantum dots to agglomerate. The acetone and methanol were removed, and the quantum dots were then exposed to water in the same manner as during the vacuum-removal process.

2.7 Characterization

2.7.1 UV-Visible Spectroscopy

A sample of DHLA-functionalized quantum dots dissolved in methanol and DDT-capped quantum dots dissolved in toluene was analyzed using a Cary 300 Bio UV-Visible Spectrophotometer. The solutions were analyzed from 800 nm to 300 nm using baseline correction with pure methanol or toluene.

2.7.2 Photoluminescence

The samples analyzed using UV-visible spectroscopy were also excited to measure photoluminescence. Data was collected using a Horiba Jobin Yvon FL-1039/40 450 Watt Illuminator with an excitation wavelength of 450±1.0 nm as determined from the location of the first excitation observed during UV-visible spectroscopy. Emission was detected from 455-800 nm in increments of 0.5 nm. Data was normalized with respect to a standard rhodamine 6G (R6G) dye suspended in ethanol know to have 95% quantum yield.

2.7.3 Raman Spectroscopy

Raman spectroscopy was performed on quantum dot samples prepared by evaporating the quantum dot solution on a glass slide. Both DHLA- and DDT-capped quantum dot samples were prepared so only quantum dots and capping ligands remained on the slide after the solvent had been removed. Characterization was

performed using a Horiba Jobin Yvon LabRAM HR Raman system with an Olympus BX41 microscope and a 325-nm Kimmon IK Series He-Cd Laser. An 800-µm hole size was used to collect data from 200-2000 cm^{-1}. Spectra were collected in two 14-second acquisitions.

3 Results and Discussion

3.1 Outcomes

Ligand exchange reactions as described in this report are stable, well-understood reactions that enjoy a high success rate. Results were repeatable, and the procedure was updated over time to improve performance by adding additional hexane to counteract evaporation, decreasing the lipoic acid (LA) concentration to reduce material usage and reduce an excess of LA thought to hinder isolation efforts, and improving the washing process used following the reaction to create a more pure, concentrated product (see **Appendix A** for full procedure).

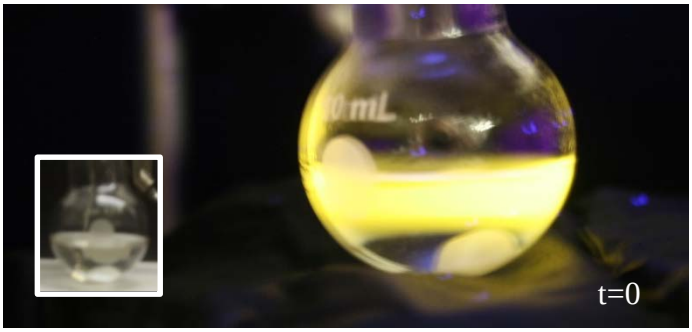

Figure 8: Images showing the ligand exchange reaction prior to commencing stirring. The main image pictures the reaction under UV light with dodecanethiol-capped (DDT-capped) quantum dots soluble in hexane. The bottom layer is 50 mM LA in methanol. The inset shows the reaction precursors in ambient light.

The exact conditions necessary for each ligand exchange reaction will vary slightly based on the concentration of quantum dots used and the degree of exchange desired (e.g. most or all quantum dots transferred into methanol). The reaction can take place with LA concentration between 50 mM and 100 mM. A wider range may be possible, but 10 mM LA is known to be too dilute. Similarly, different amounts of hexane could be added to the concentrated quantum dot precursor. Adding additional hexane counteracts the effects of evaporation and prevents agglomeration on the

walls of the reaction vessel. The reaction was stable when adding between 1200-µL and 2000-µL pure hexane to 300-µL concentrated quantum dots in hexane. **Figure 8** shows the appearance of the reaction vessel under both UV (main image) and ambient light (inset) prior to turning on the stirrer and commencing the reaction. The dodecanethiol-functionalized (DDT-functionalized) quantum dots are visible in the hexane layer which rests on top of the methanol phase containing 50 mM LA.

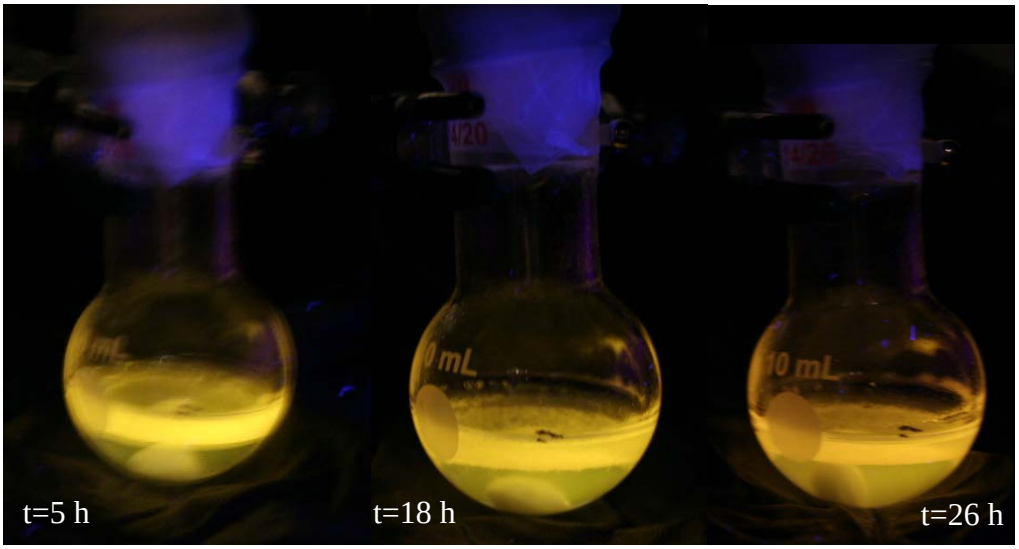

Figure 9: Pictures showing ligand exchange reaction progress at 5, 18, and 26 hours. More quantum dots are transferred into the LA-containing methanol phase in each image showing the progress of the reaction. The reaction could be ended after only 5 hours, but they are generally allowed to progress 24-48 hours to obtain a greater degree of ligand exchange.

The ligand exchange reaction was commonly left for 24-48 hours to allow an acceptable amount of ligand exchange to occur. **Figure 9** shows three stages in the reaction to display the typical exchange progression. Exchange begins to occur almost immediately and is fully detectable after approximately 5 hours as demonstrated in the leftmost image. The reaction could be ended at this point if only a small amount of exchange was desired, but the most difficult parts of the ligand exchange process are the preparation and purification providing an incentive to allow the reaction to continue. The second two images show the reaction after 18 and 26 hours. Ligand

exchange has occurred to a greater extent as evidenced by stronger luminescence in the methanol-phase and a more dilute hexane phase. Quantum dots begin to agglomerate on the flask walls due to evaporation as described in **Figure 7**.

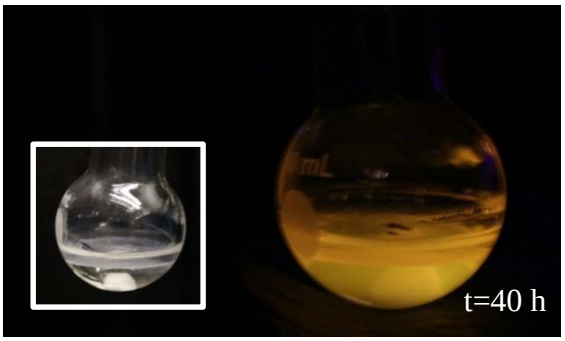

Figure 10: Image of reaction vessel after 40 hours of reaction time. The ligand exchange reaction was stopped at this point because an acceptable amount of exchange had occurred. Hexane evaporation (as described in **Figure 7**) is evident when compared to **Figure 8**. The inset image, taken under ambient light, shows the presence of a precipitate in the hexane phase while the methanol phase remained clear.

Ligand exchange reactions were allowed to progress until the majority of quantum dots had been transferred into methanol and appreciable progress was no longer being made as determined by a visual inspection. This criterion is subjective and can be adjusted based on the purpose of the reaction, time constraints, and research needs. Reaction time will also be affected by the concentration of quantum dots originally used and the concentration of LA. Increased quantities of LA will allow the reaction to proceed more quickly and to a greater extent, but excess LA not reduced to dihydrolipoic acid (DHLA) can damage the product. **Figure 10** pictures the reaction at its completion after approximately 40 hours. Hexane evaporation as described in **Figure 7** can be observed when the image is compared to **Figure 8**, and the inset image taken in ambient light shows a precipitate formed in the hexane phase while the methanol phase remained clear. Reaction success was confirmed by centrifuging the unwashed methanol phases at high speeds (i.e. 13500 rpm) for 60 minutes without observing any quantum dot precipitation.

Figure 11: Image showing quantum dots dissolved in methanol prior to removing the last portion of wash hexane. The solution became more concentrated each time it was washed with hexane, as a small amount of methanol is soluble in hexane.

The washing process described in **Materials and Methods** and **Appendix A** produces high-quality concentrated quantum dots soluble in methanol. A typical product is pictured in **Figure 11** prior to removal of the final portion of wash hexane. The washing process requires great care because of some procedural difficulties. Extra care is needed when removing the supernatant following centrifugation because the precipitate on the walls of the vial is easily resuspended preventing impurities from being removed. Wash hexane also must be added with care, as it forms a binary mixture with some of the methanol reducing the amount available for quantum dots to remain in solution. Adding too much hexane will cause the quantum dots to precipitate.

3.2 Characterization

3.2.1 UV-Visible Spectroscopy

UV-visible spectroscopy was conducted to determine the absorbance of the methanol-soluble, DHLA-capped quantum dots and the corresponding toluene-soluble, DDT-capped precursor. Quantum dots in methanol absorbed 1.6% of 450-nm UV radiation while toluene-soluble quantum dots absorbed 1.0 % of the same radiation. Greater absorbance corresponds to a higher quantum dot concentration in

the sample. Relative quantum dot concentration is needed to normalize photoluminescence data and determine quantum yield.

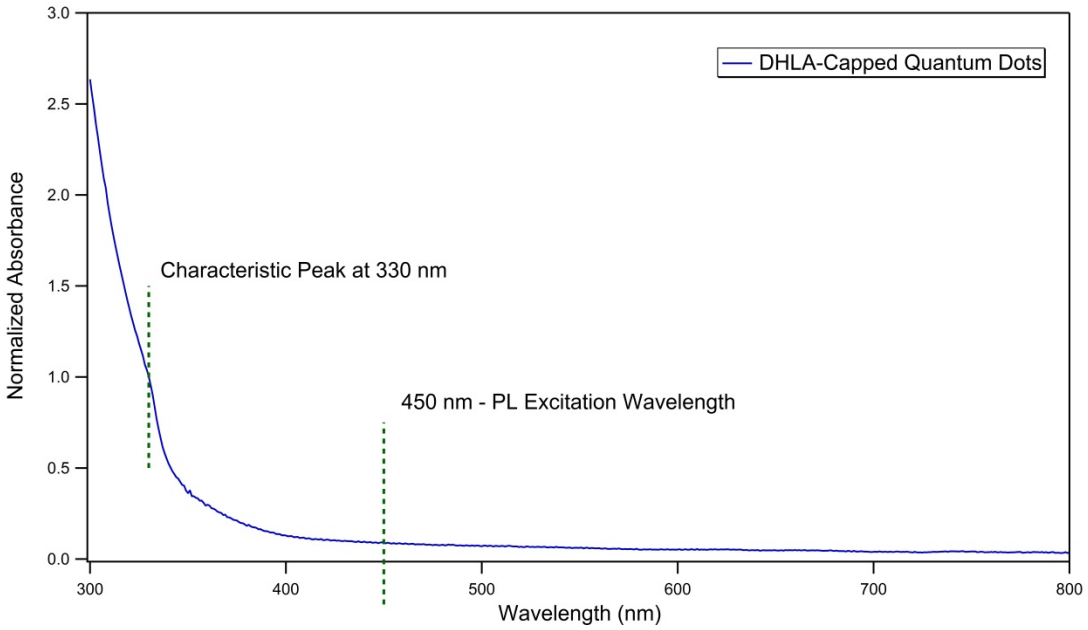

Figure 12: UV-visible spectrum for DHLA-capped quantum dots dissolved in methanol. Absorbance is normalized to the characteristic band edge peak at 330 nm. The quantum dots absorbed 1.6% of UV radiation at 450-nm, the photoluminescence excitation wavelength. A comparison to DDT-capped quantum dots is available in **Appendix B**.

Figure 12 shows the spectrum collected for methanol-soluble quantum dots. Absorbance data has been normalized to the band edge characteristic peak located at 330 nm. **Appendix B** displays data comparing the methanol- and toluene-soluble quantum dots. Toluene absorbs UV radiation in the 300-350 nm range causing the increased absorbance that interferes with the desired signal.

3.2.2 Photoluminescence

Photoluminescence data was numerically integrated and normalized to account for solvent selection and quantum dot concentration to determine the quantum yield of the methanol-soluble product and the toluene-soluble precursor. Data was normalized with respect to the maximum intensity and smoothed to remove noise.

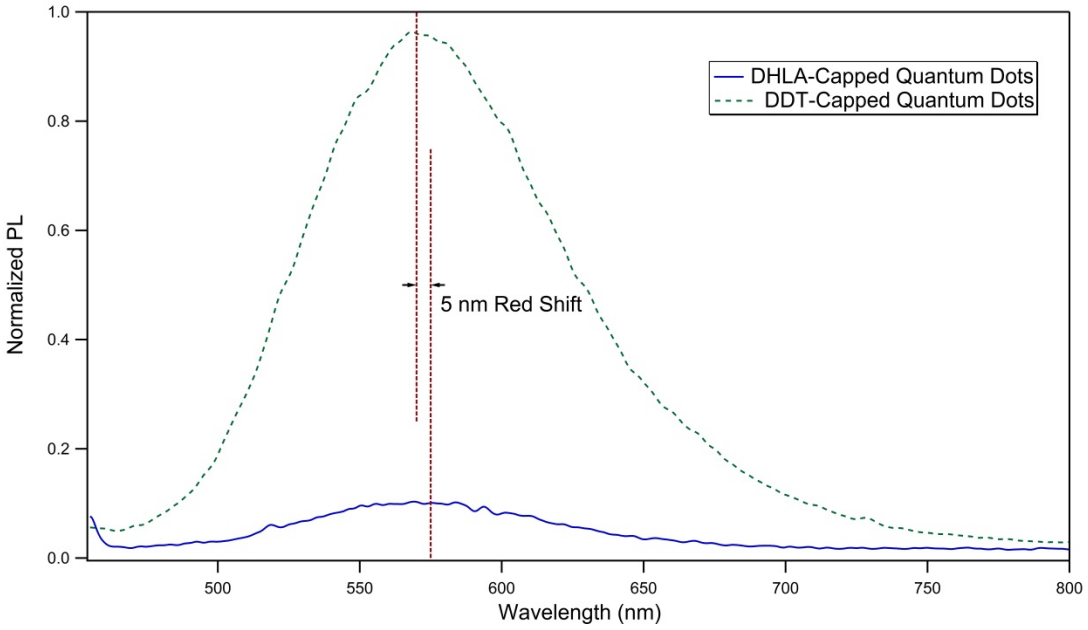

Figure 13: Photoluminescence spectra for the DHLA-capped ligand exchange product (blue) and DDT-capped precursor (green). A 5-nm red shift in peak location was observed similar to literature reports. Quantum yield was calculated by comparing peak areas to a known standard with 95% quantum yield. Quantum yield decreased approximately 90% after ligand exchange from 24.6% to 2.8%. Literature reports document similar decreases in quantum yield following ligand exchange. Quantum yield calculations are detailed in **Appendix C**.

Quantum yield for the ligand exchange product was determined to be 2.8% while the DDT-capped precursor had a quantum yield of 24.6% when excited at 450±1.0 nm. The photoluminescence spectra can be seen in **Figure 13** where the product is shown by the blue trace, and the precursor is represented by the green trace. Quantum yield calculations are detailed in **Appendix C**. The location of peak photoluminescent intensity red shifted approximately 5 nm, similar to values reported in the literature. [1] [6] [10] The 90% decrease in quantum yield is higher than several values reported but equivalent to others indicating a large loss of quantum yield should be expected following ligand exchange. [1] [2] [3] [5] [6] [7] [8] [10] [13] [16] [18] The decrease in quantum yield during ligand exchange is suspected to be due to loss of material quality because of aging, exposure to oxygen, or interaction with byproducts and excess LA. There is some evidence in literature to suggest that the

exact identity of the ligand, its concentration, and the number of binding sites (i.e. monodentate or multidentate) can affect the drop in quantum yield. [7] [13] [16]

3.2.3 Raman Spectroscopy

Raman spectroscopy was conducted to observe any differences between DHLA- and DDT-capped quantum dots and to provide additional evidence of successful ligand exchange. DDT and DHLA are expected to have different interactions with the quantum dot surface due to the presence of an additional thiol group in DHLA (see **Figure 4**). DDT is a straight-chain molecule with a terminal thiol group.

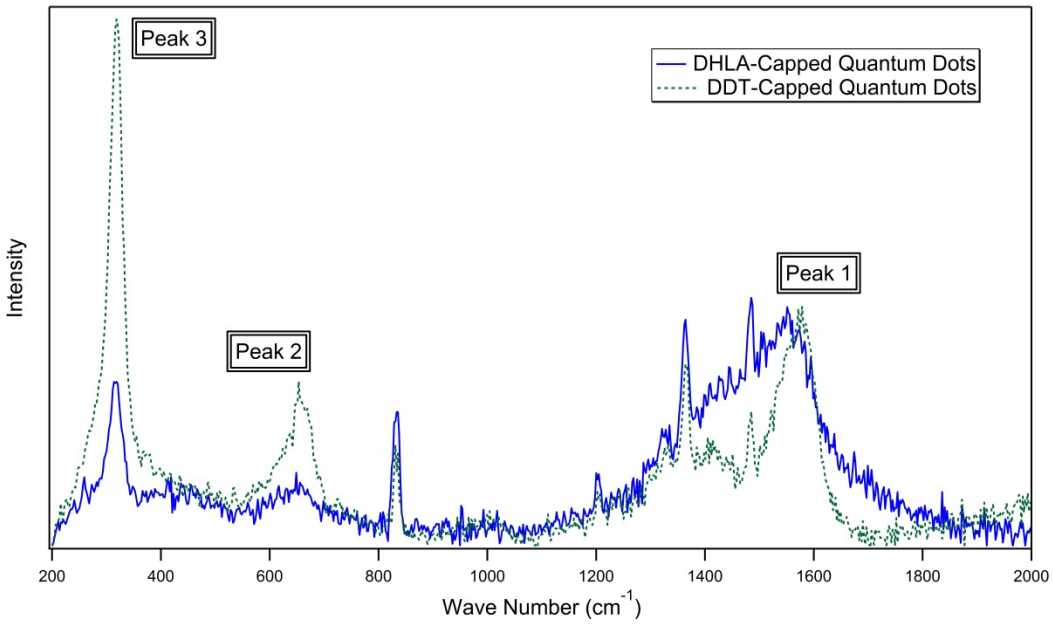

Figure 14: Raman spectra displaying DHLA-capped quantum dots using a blue trace and DDT-capped quantum dots with a green trace. Peak 1 is significantly larger for DHLA-capped quantum dots that possess two thiol groups. This peak represents an increase in R-SH scissoring. Peak 2 shows the amount of C-S stretching for both samples. The DDT-capped precursor displays a larger peak because DDT possesses a long alkane backbone. The shorter backbone of DHLA produces less stretching. The ZnS shells of the quantum dots produce Peak 3. DHLA-capped quantum dots have a smaller peak because of excess LA in the analyzed sample. The DDT-capped precursor was exceptionally pure and displayed a larger peak. Additional peaks are due to the alkane backbones of the ligands and R-SH wagging that both exhibit.

The Raman spectra in **Figure 14** displays the differences between the DDT-capped precursor in green and the DHLA-capped ligand exchange product in

blue. The broad peak present around 1600 cm^{-1} is significantly larger for DHLA-capped quantum dots that possess two thiol groups (Peak 1 in **Figure 14**). The larger peak represents an increase in R-SH scissoring due to the additional thiol group. Another characteristic difference is seen around 650 cm^{-1} (Peak 2 in **Figure 14**). This peak represents the C-S stretch between the alkane backbone and the thiol group. This peak is larger for the DDT-capped precursor because of its straighter and longer alkane backbone. DHLA forms by ring opening and has a structure with more branching and a shorter alkane backbone causing less C-S stretching to be detected (see structure in **Figure 4**). All other peaks were essentially identical between the precursor and product with the exception of the Peak 3 in **Figure 14** centered around 325 cm^{-1} which is caused by detection of the ZnS shell. Excess LA present in the DHLA-capped sample reduced the size of this peak in relation to the exceedingly pure DDT-capped sample. An additional peak from the terminal carboxylic acid group on DHLA was not visible through the noise of Raman photoluminescence around 3575 cm^{-1} (not shown in **Figure 14**). [19]

3.3 Challenges

The isolation phase of the ligand exchange process has proven to be especially challenging for $CuInS_2$-ZnS quantum dots. DHLA-capped quantum dots have not been successfully transferred into water despite the continuing success and improvement of the ligand exchange reaction which uses methanol as the polar solvent. Two different isolation schemes have been attempted in addition to performing checks to ensure the quantum dots were actually soluble, not just suspended, in methanol.

Most effort has been directed toward transferring the quantum dots into water by evaporating methanol under vacuum as suggested in the literature. [1] [7] [18] Filtered 18.2-MΩ deionized water was then added to attempt to dissolve the quantum dots, but they would remain aggregated even after sonication. Another approach also vacuumed away methanol before adding in deionized water adjusted to pH 9-10 using sodium hydroxide. Quantum dot aggregation was even more apparent in this case. Adding a basic solution was intended to encourage deprotonation (and subsequent solubility) of the terminal carboxylic acid groups on DHLA that may occur more easily in methanol than water (see **Figure 4** for an image of deprotonated DHLA). [1] [6] [12] [18]

An attempt was also made to isolate the quantum dots from methanol by using a large excess of acetone to “crash” them out of solution. [2] [3] [5] Acetone interacted with DHLA disrupting its solubility in methanol and initiating agglomeration. The excess acetone and methanol were then removed and filtered deionized water was added. The result was similar to the vacuum processes. **Table 2** provides a summary of isolation methods used in the literature reviewed to develop these procedures.

Table 2: Summary of several isolation processes following ligand exchange. The ligand used and information regarding further functionalization are listed. "Vacuum" refers to solvent removal by vacuum, "Base" refers to adjusting the solution pH, "Crashing" refers to precipitation using acetone, and "Separation" refers to a physical separation process.

Ligand	Functionalization	Process	Source
LA/DHLA-based	Polyethylene glycol (PEG)-OCH_3, PEG-COOH, PEG-NH_2, and zwitterion	Vacuum, Base	[1]
3-mercaptopropionic acid (MPA)	No additional functionalization	Crashing, Separation	[5]
LA/DHLA	PEG	Base	[6]
LA/DHLA	Maltose binding protein	Base	[12]
LA/DHLA-based	Zwitterion and triethylene glycol zwitterion	Vacuum	[7]
Bis(LA)/Bis(DHLA)	Zwitterion, -NH_2, -COOH	Vacuum	[18]
11-mercaptoundecanoic acid (MUA)	No additional functionalization	Crashing	[2]
MPA	No additional functionalization	Crashing	[3]
LA/DHLA or MUA	2A3 and EG2	Separation	[8]

Several possible causes could account for the insolubility of quantum dots in water, but ligand exchange failure has been ruled out. Quantum dots were successfully redissolved in methanol following removal of the original methanol by evaporation. Solubility persisted even after centrifugation at high speeds (i.e. 13500 rpm for 30 minutes). The suspected causes for insolubility in water include byproduct polymerization or lower solubility of DHLA in water than in methanol. Excess LA remaining in solution could be initiating a polymerization reaction upon removal of methanol that propagates to include DHLA ligands attached to quantum dots. This encourages formation of S-S bonds (see **Figure 4** for chemical structures) which water is unable to break when added to the quantum dots (methanol is able to solubilize the quantum dots). Water solubility may also be affected by the solubility limit of LA/DHLA which is more soluble in methanol than in water. [20] Water solubility issues have been reported for some functionalized DHLA-capped quantum dots even though they were soluble in polar organic solvents such as methanol or ethanol. [6]

4 Conclusions and Recommendations

4.1 Conclusions

Lipoic acid (LA) was reduced to dihydrolipoic acid (DHLA) and ligand exchange with dodecanethiol-capped $CuInS_2$-ZnS core-shell quantum dots occurred. The reaction was allowed to proceed 24-48 hours when using 50 mM LA in methanol and quantum dots dissolved in hexane. Reaction success was confirmed by continued solubility of quantum dots in methanol following high-speed centrifugation. The product was characterized using UV-visible spectroscopy, photoluminescence, and Raman spectroscopy. Quantum yield decreased from approximately 25% to 3% and a 5-nm red shift in peak location was observed after ligand exchange. Challenges were encountered when trying to transfer quantum dots to water using vacuum evaporation and acetone “crashing” strategies. Proposed causes include polymerization of excess LA or LA/DHLA solubility limits in water. The process described shows great promise for producing non-toxic, water-soluble quantum dots for biological and non-biological applications. Many non-biological applications are already feasible at this time using the quantum dots as prepared in methanol. Theory indicates that the methanol-soluble quantum dots obtained should be transferrable into water or other polar solvents.

4.2 Recommendations for Future Work

Future work in the short term will focus on transferring the DHLA-capped quantum dots into water. Efforts will first be focused on acetone “crashing,” as it was only tried once previously. This method also deserves further consideration as it

allows for the removal of all excess LA and other byproducts soluble in both polar and nonpolar phases. Further study of this method is needed to determine whether it will work for this $CuInS_2$-ZnS system. Dissolving quantum dots in water adjusted to have a low pH should also be attempted. Acidic conditions are intended to shift the equilibrium of the LA reduction ensuring as much DHLA remains as possible to encourage water solubility (see **Figure 4**). A ligand exchange reaction should also be conducted using only $CuInS_2$ quantum dot cores not encapsulated by shells. This could improve the ligand exchange process by providing additional electrons to drive LA reduction through UV excitation of the semiconductor core (for $CuInS_2$, E_{BG}≈1.5 eV=827 nm) which is hindered by the presence of a high band gap shell (for ZnS, E_{BG}≈3.5 eV=355 nm). A faster exchange reaction could eliminate issues with solvent evaporation and allow the reaction to proceed to a greater extent in less time than for core-shell quantum dots. A different surface may also provide more favorable interactions with ligands and encourage water solubility. Usage of different solvents could also be explored to improve the process and encourage full transfer to water (e.g. ethanol could be evaporated away after the addition of water). Direct ligand exchange into water could also be explored.

Another important goal is improved quantum yield. The significant drop in quantum yield currently experienced may increase with further functionalization and make any imaging applications impractical. Other groups have reported as much as 70% of quantum yield can be retained following ligand exchange. [1] [6] [7] [18] One possible method for improving quantum yield is removal of excess LA that could be interfering with UV absorption. This suggests that acetone “crashing” may be the best

quantum dot isolation strategy to pursue. Another area to study is ligand exchange reaction yield. The percentage of quantum dots transferred from hexane into methanol and then into water could be determined using thermal gravimetric analysis to remove all organic components and analyze only the amount of inorganic quantum dots present in a sample. A better understanding of reaction yield would allow precursor concentrations and reaction conditions to be optimized.

Long-term studies will focus on functionalization of and applications for water-soluble quantum dots. A critical portion of this phase will be toxicity tests to study the effects of the DHLA-capped quantum dots on life. All materials were selected to be biocompatible, but impurities from the exchange and purification processes may remain indicating greater care will be needed in purification and isolation. Experiments will be conducted to functionalize the DHLA-capped quantum dots beginning with polyethylene glycol. Further reactions with antibodies or other functional groups can be pursued in conjunction with life science researchers who have experience in targeting specific tissues within the body. Non-biological applications can also be pursued including producing a water- or polar solvent-based quantum dot “ink” that can be used to print features for photovoltaic, LED, or other quantum dot applications.

Works Cited

[1] G. Palui, T. Avellini, N. Zhan, F. Pan, D. Gray, I. Alabugin and H. Mattoussi, "Photoinduced Phase Transfer of Luminescent Quantum Dots to Polar and Aqueous Media," *Journal of the American Chemical Society,* vol. 134, no. 39, pp. 16370-16378, 2012.

[2] W. Zhang and X. Zhong, "Facile Synthesis of ZnS-$CuInS_2$-Alloyed Nanocrystals for a Color-Tunable Fluorchrome and Photocatalyst," *Inorganic Chemistry,* vol. 50, no. 9, pp. 4065-4072, 2011.

[3] W. Zhang, G. Chen, J. Wang, B.-C. Ye and X. Zhong, "Design and Synthesis of Highly Luminescent Near-Infared-Emitting Water-Soluble CdTe/CdSe/ZnS Core/Shell/Shell Quantum Dots," *Inorganic Chemistry,* vol. 48, no. 20, pp. 9723-9731, 2009.

[4] P. V. Kamat, "Quantum Dot Solar Cells. The Next Big Thing in Photovoltaics," *The Journal of Physical Chemistry Letters,* vol. 4, no. 6, pp. 908-918, 2013.

[5] C.-C. Chang, J.-K. Chen, C.-P. Chen, C.-H. Yang and J.-Y. Chang, "Synthesis of Eco-Friendly $CuInS_2$ Quantum Dot-Sensitized Solar Cells by a Combined Ex Situ/in Situ Growth Approach," *Applied Materials and Interfaces,* vol. 5, no. 21, pp. 11296-11306, 2013.

[6] H. T. Uyeda, I. L. Medintz, J. K. Jaiswal, S. M. Simon and H. Mattoussi, "Synthesis of Compact Multidentate Ligands to Prepare Stable Hydrophilic Quantum Dot Fluorophores," *Journal of the American Chemical Society,* vol. 127, no. 11, pp. 3870-3878, 2005.

[7] N. Zhan, G. Palui, H. Grise, H. Tang, I. Alabugin and H. Mattoussi, "Combining Ligand Design with Photoligation to Provide Compact, Colloidally Stable, and Easy to Conjugate Quantum Dots," *Applied Materials & Interfaces,* vol. 5, no. 8, pp. 2861-2869, 2013.

[8] K. Yu, P. Ng, J. Ouyang, M. B. Zaman, A. Abulrob, T. N. Baral, D. Fatehi, Z. J. Jakubek, D. Kingston, X. Wu, X. Liu, C. Hebert, D. M. Leek and D. M. Whitefield, "Low-Temperature Approach to Highly Emissive Copper Indium Sulfide Colloidal Nanocrystals and Their Bioimaging Applications," *Applied Materials & Interfaces,* vol. 5, no. 8, pp. 2870-2880, 2013.

[9] T. Pons, E. Pic, N. Lequeux, E. Cassette, L. Bezdetnaya, F. Guillemin, F. Marchal and B. Dubertret, "Cadmium-Free $CuInS_2$/ZnS Quantum Dots for Sentinel Lymph Node Imaging with Reduced Toxicity," *ACS Nano,* vol. 4, no. 5, pp. 2531-2538, 2010.

[10] J. Schornbaum, Y. Zakharko, M. Held, S. Thiemann, F. Gannott and J. Zaumseil, "Light-Emitting Quantum Dot Transistors: Emission at High Charge Carrier Densities," *Nano Letters,* vol. 15, no. 3, pp. 1822-1828, 2015.

[11] H. S. Choi, W. Liu, P. Misra, E. Tanaka, J. P. Zimmer, B. I. Ipe, M. G. Bawendi and J. V. Frangioni, "Renal clearance of quantum dots," *Nature Biotechnology,* vol. 25, no. 10, pp. 1165-1170, 2007.

[12] H. Mattoussi, J. M. Mauro, E. R. Goldman, G. P. Anderson, V. C. Sundar, F. V. Mikulec and M. G. Bawendi, "Self-Assembly of CdSe-ZnS Quantum Dot Bioconjugates Using an Engineered Recombinant Protein," *Journal of the American Chemical Society,* vol. 122, no. 49, pp. 12142-12150, 2000.

[13] B.-K. Pong, B. L. Trout and J.-Y. Lee, "Modified Ligand Exchange for Efficient Solubilization of CdSe/ZnS Quantum Dots in Water: A Procedure Guided by Computational Studies," *Langmuir,* vol. 24, no. 10, pp. 5270-5276, 2008.

[14] M. Bottrill and M. Green, "Some aspects of quantum dot toxicity," *Chemical Communications,* vol. 47, no. 25, pp. 7039-7050, 2011.

[15] W. R. Algar, K. Susumu, J. B. Delehanty and I. L. Medintz, "Semiconductor Quantum Dots in Bioanalysis: Crossing the Valley of Death," *Analytical Chemistry,* vol. 83, no. 23, pp. 8826-8837, 2011.

[16] Y. Zhang and A. Clapp, "Overview of Stabilizing Ligands for Biocompatible Quantum Dot Nanocrystals," *Sensors,* vol. 11, no. 12, pp. 11036-11055, 2011.

[17] K. P. Shay, R. F. Moreau, E. J. Smith, A. R. Smith and T. M. Hagen, "Alpha-lipoic acid as a dietary supplement: Molecular mechanisms and therapeutic potential," *Biochimica et Biophysica Acta - General Subjects,* vol. 1790, no. 10, pp. 1149-1160, 2009.

[18] N. Zhan, G. Pauli, M. Safi, X. Ji and H. Mattoussi, "Multidentate Zwitterionic Ligands Provide Compact and Highly Biocompatible Quantum Dots," *Journal of the American Chemical Society,* vol. 135, no. 37, pp. 13786-13795, 2013.

[19] D. Lin-Vien, N. B. Colthup, W. G. Fateley and J. G. Grasselli, The Handbook of Infrared and Raman Characteristic Frequencies of Organic Molecules, San Diego, CA: Academic Press, Inc., 1991.

[20] Toxicology Data Network, "HSDB: Alpha-Lipoic Acid," U.S. National Library of Medicine, 4 January 2011. [Online]. Available: http://toxnet.nlm.nih.gov/cgi-bin/sis/search2/f?./temp/~cNrgCa:1. [Accessed 18 May 2015].

[21] B. C. Fitzmorris, Y.-C. Pu, J. K. Cooper, Y.-F. Lin, Y.-J. Hsu, Y. Li and J. Z. Zhang, "Optical Properties and Excition Dynamics of Alloye Core/Shell/Shell $Cd_{1-x}Zn_xSe$/ZnSe/ZnS Quantum Dots," *Applied Materials & Interfaces,* vol. 5, no. 8, pp. 2893-2900, 2013.

[22] Louisana State University, "Refractive Index," [Online]. Available: macro.lsu.edu/HowTo/solvents/Refractive%20Index.htm. [Accessed 21 May 2015].

Appendix A Lipoic Acid Ligand Exchange Procedure

1. Transfer lipoic acid (LA), concentrated quantum dots, reaction vessel, stir bar, waste container, auto pipette, and consumables (spatula, weighing paper, pipette tips, septums) into the glove box. Turn on glove box light.
2. Prepare 1000-µL 50 mM LA in methanol inside the glove box. Ensure the mixture is homogeneous.
    a. Prepare 1000-µL 100 mM LA in methanol.

    $$1000\ \mu\text{L solution}\left(\frac{10^{-6}\ \text{L}}{\mu\text{L}}\right)\left(\frac{100\ \text{mmole}}{\text{L}}\right)\left(\frac{206.33\ \text{mg}}{\text{mmole}}\right) 20.633\ \text{mg LA}$$

    b. Combine 500-µL 100 mM LA with 500-µL methanol and add to flask.
3. Add 2000-µL hexane to the one-neck flask then add 300-µL concentrated quantum dots in hexane (amount may vary depending on how concentrated the quantum dots are). Add a stir bar to the flask, and attach a septum.
4. Transfer the reaction vessel, LA bottle, and concentrated quantum dots out of the glove box (remove any waste). Seal bottles with paraffin film to reduce the chances of oxygen exposure.
5. Irradiate with hand held UV lamp for 24-48 hours. The flask should be suspended above a stirrer allowing for vigorous stirring during the reaction.

6. Transfer flask back into glove box (also transfer in three centrifuge vials and several Pasteur pipettes). Remove and discard hexane phase and transfer methanol phase with quantum dots into centrifuge vial. Add hexane and shake. Centrifuge for 3 minutes at 3000 rpm to wash the product and remove dodecanethiol ligands.
7. Discard hexane phase. Withdraw methanol phase and transfer to clean centrifuge vial. Discard any remaining precipitate. Volume of methanol phase may decrease because a binary mixture is formed with hexane (no quantum dots are lost to this binary mixture).
8. Repeat steps 7 and 8 to wash quantum dots in methanol three times.
9. Perform further isolation steps to dissolve quantum dots in water.

Appendix B Additional UV-Visible Spectroscopy Data

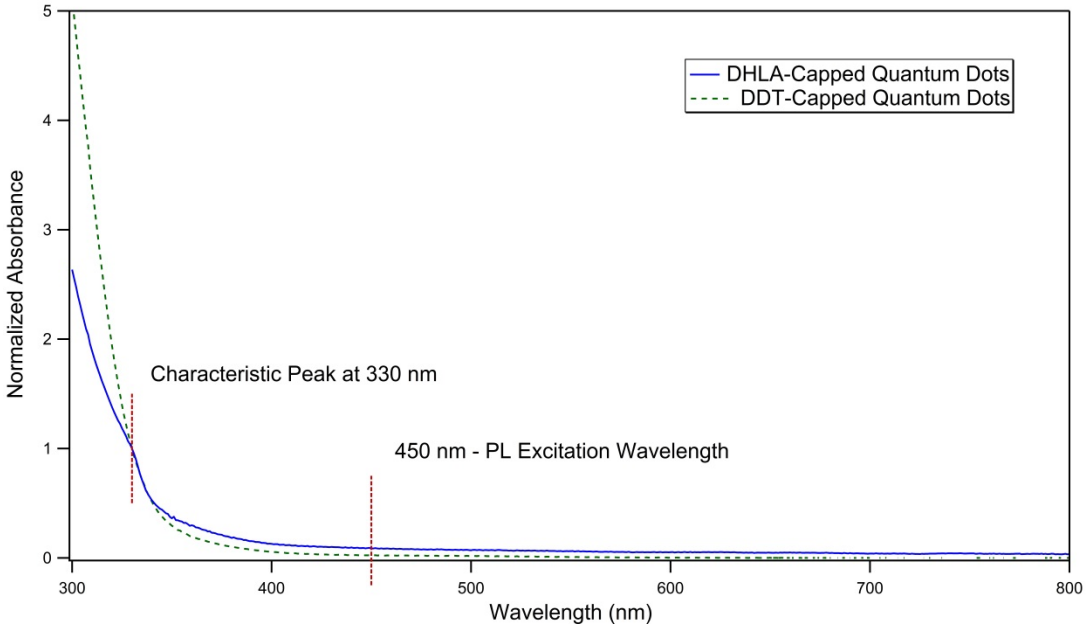

Figure 15: UV-visible spectra for quantum dots dissolved in methanol and toluene normalized with respect to the band edge characteristic peak at 330 nm. The wide shoulder for dodecanethiol-capped quantum dots is due to the absorbance of toluene in the 300-350 nm range. Prior to this region the spectra are almost identical.

Appendix C Quantum Yield Calculations

Quantum yields were calculated using numerical integration and normalization against a known standard. The area under each peak in **Figure 13** was calculated using the trapezoid rule with a data point every 0.5 nm from 455 nm to 800 nm (**Eq. 1**). Each data point was corrected for relative concentration by dividing by the absorbance at 450 nm determined using UV-visible spectroscopy before calculating the sum (see **Figure 12**).

$$A = \sum_{m} (\lambda_{m+1} - \lambda_m) \frac{(I_{m+1} + I_m)}{2} \qquad \textbf{(Eq. 1)}$$

The total area for both dihydrolipoic acid-capped (DHLA-capped) quantum dots and dodecanethiol-capped (DDT-capped) quantum dots was compared to instrument response for a standard solution of rhodamine 6G (R6G) dye suspended in ethanol that was known to have 95% quantum yield. (**Eq. 2**) which is used to calculate quantum yield also corrects for solvent indices of refraction. [21]

$$QY = QY_{\text{standard}} \frac{A_{\text{QD}}}{A_{\text{standard}}} \frac{n_{\text{QD solvent}}}{n_{\text{standard solvent}}} \qquad \textbf{(Eq. 2)}$$

A sample of trapezoid-rule area calculations is displayed in **Table 3** while a summary of quantum yield calculations is displayed in **Table 4**. Each intensity data point for DHLA-capped quantum dots was divided by 1.6% (UV-visible absorption at 450 nm) to correct for concentration. Data points for DDT-capped quantum dots were divided by 1.0%. The DHLA-capped product had a calculated area of 1.04×10^7 arbitrary units (AU), and the DDT-capped precursor had an area of 8.10×10^7 AU. The R6G dye had an area of 3.44×10^8 AU.

Table 3: Table displaying a sample of trapezoidal-rule area calculations to determine quantum yield. Each DHLA-capped quantum dot intensity data point was corrected by dividing by the 1.6% UV-visible absorbance at 450 nm, and each DDT-capped quantum dot intensity data point was divided by 1.0%. Total areas were 1.04×10^7 AU for DHLA-capped quantum dots and 8.10×10^7 AU for DDT-capped quantum dots. R6G dye had an area of 3.44×10^8 AU.

Wavelength (nm)	DHLA-Capped Quantum Dots in Methanol			DDT-Capped Quantum Dots in Toluene		
	Intensity (AU)	Corrected (AU)	Trapezoidal Area (AU)	Intensity (AU)	Corrected (AU)	Trapezoidal Area (AU)
455	31118	19487	34930	11712	11289	21383
455.5	24661	15443	28073	10473	10094	19590
456	20168	12630	23604	9852	9495	17967
456.5	17526	10975	18618	8790	8472	17930
457	12205	7643	15215	9814	9459	19000
457.5	12093	7573	14921	9900	9542	18260
458	11735	7348	13784	9046	8719	17100
458.5	10277	6436	10572	8696	8381	17121
459	6605	4136	9311	9068	8740	18655
459.5	8263	5175	11068	10288	9916	21862
460	9411	5893	9790	12395	11947	19994
⋮	⋮	⋮	⋮	⋮	⋮	⋮
799.5	3727	2334	4776	6002	5785	10431

Table 4: Calculations using **(Eq. 2)** to calculate quantum yield. Indices of refraction are 1.33 for methanol, 1.36 for ethanol, and 1.50 for toluene. [22] DHLA-capped quantum dots had a quantum yield of 2.8% while DDT-capped quantum dots had a quantum yield of 24.6%.

DHLA-Capped QD in Methanol	$(95\%)\left(\frac{1.04\times10^7}{3.44\times10^8}\right)\left(\frac{1.33}{1.36}\right)$	2.8%
DDT-Capped QD in Toluene	$(95\%)\left(\frac{8.10\times10^7}{3.44\times10^8}\right)\left(\frac{1.50}{1.36}\right)$	24.6%

Appendix D List of Abbreviations

Abbreviation	Meaning
ACS	American Chemical Society
AU	Arbitrary units
DDT	Dodecanethiol
DHLA	Dihydrolipoic acid
HPLC	High Performance Liquid Chromatography
LA	Lipoic acid
LED	Light-emitting diode
MPA	3-mercaptopropionic acid
MUA	11-mercaptoundecanoic acid
PEG	Polyethylene glycol
TOP	Trioctylphosphine
TOPO	Trioctylphosphine oxide
UV	Ultraviolet